Oxygen Adsorption on (111)-Oriented Diamond: A Study with Ultraviolet Photoelectron Spectroscopy, Temperature-Programmed Desorption, and Periodic Density Functional Theory

Kian Ping Loh,* X. N. Xie, S. W. Yang, and J. C. Zheng

Department of Chemistry, National University of Singapore, Lower Kent Ridge Road, Singapore 119260

Received: October 25, 2001; In Final Form: January 30, 2002

Using ultraviolet photoelectron spectroscopy (UPS), temperature programmed desorption (TPD), and periodic density functional theory (DFT), we have investigated the oxidation chemistry of diamond (111) surface following its exposure to atomic oxygen generated from a remote radio frequency discharge. Partial O uptake occurs on the C(111) 2 × 1 surface at room temperature without lifting the surface reconstruction. A 2 × 1 → 1 × 1 transition and a full monolayer O coverage is only achieved following the oxygenation of the diamond surface at elevated temperatures (400 °C). Exchange of chemisorbed D by atomic O, and vice versa, is facile at room temperature. Desorption products originating from the reaction chemistry between O and D such as D_2O were observed on the C(111) surface in addition to CO. The C(111) surface is readily graphitized following the desorption of CO from the surface. In addition, the structure and energetics of oxygenated C(111) 1 × 1 and C(111) 2 × 1 surfaces have been studied using periodic density functional theory (DFT). The oxidation processes have been examined in terms of the reaction heats. The calculations revealed that the epoxy configuration formed by bridging O on the Pandey chain is more stable at low O coverage, these converted to a carbonyl-type oxygen species at higher coverages. Reaction heat considerations suggest that hydroxyl-terminated C(111) 1 × 1 may be the final stable product in the presence of atomic hydrogen.

1. Introduction

The study of the interaction of oxygen with diamond surfaces is important from the perspective of understanding the effects of oxygen on the low-temperature growth of diamond[1,2] as well as controlling its surface electronic and chemical properties by varying the surface functional groups.[3,4] The addition of oxygen into the CVD plasmas has been found to lower the growth temperatures and enhance the crystalline quality of chemical vapor deposited diamond.[1,2] This may come about from the enhanced surface etching of nondiamond sp^2 phases by atomic O, or through the higher regeneration of surface radical sites by O ion abstraction of surface H during CVD, although the detailed mechanism is not understood. The surface electronic properties of diamond may be tuned by creating spatially resolved domains of oxygen or hydrogen, which can produce opposing influences on its electron affinity and surface conductivity, the latter two properties being the most critical in the applications of diamond as electron emitters and transistors.[3,4]

To understand the correlation between surface structure, electronic properties, and growth chemistry, it is important to investigate the reaction chemistry of hydrogen and oxygen with diamond surfaces. There have been extensive experimental and theoretical efforts looking at the interaction of hydrogen with the low index faces of diamond.[5−7] While some experimental studies have been carried out on oxygenated diamond (100)[8−11] and (110)[12] surfaces, the chemistry of oxygen with diamond (111)[13,14] surfaces has received relatively little attention. Experimental difficulties during the study of oxygenated diamond surfaces include charging problems in electron spectroscopy due to the highly insulating nature of such surfaces, and the generation of a well-characterized oxygenated diamond surface itself. Molecular oxygen has very little appreciable reaction with the inert diamond surface and increasing the pressure or substrate temperature to initiate oxidation conditions can result in the destruction of the diamond surface. Energetic oxygen species, such as ions, thermally activated oxygen molecules or reactive atoms are needed to react with active sites on the diamond surface.

Nonetheless, some progress toward understanding the nature of the chemisorbed O species on diamond surfaces has been made, although the bulk of these studies has been focused on diamond powder and the C(100) surfaces. Ando et al. investigated the chemical reaction of oxygen with diamond powder using Fourier transform infrared (FTIR) and TPD.[15] Chemisorbed functional groups such as carbonyl (C═O), lactone [(C═O)O], carboxylic acid [(C═O)OH], cyclic ether (COC), and carboxylic anhydride [(C═O)O(C═O)] were found on the diamond surfaces. Thoms et al. exposed the diamond (100) surfaces to molecular oxygen activated over a hot iridium filament and reported that atomic O could convert the reconstructed (2 × 1) surface into the (1 × 1) phase, and that CO was the dominating desorption product after annealing.[8] Hossain et al. prepared an oxygenated diamond (100) surface using the iridium activation method and applied HREELS to study the chemisorbed states of atomic O on diamond (100).[9] Pehrsson reported the observation of hydroxyl groups following the oxidation of the hydrogenated (100) surface and attributed that to oxygen insertion into C−H bonds on the surface.[10,11]

Studies on oxygenated C(111) surfaces were limited to that of R. Klauser et al. who applied a microwave plasma source to

* To whom correspondence should be directed: Dr Kian Ping Loh, FAX: (65) 779 1691, email address: chmlohkp@nus.edu.sg.

10.1021/jp0139437 CCC: $22.00
Published on Web 04/27/2002

prepare an oxygenated diamond (111) surface.[13] They reported that the surface reconstruction on C(111) 2 × 1 is not affected by O adsorption and that atomic H can replace the adsorbed O readily to convert the surface structure to 1 × 1, while atomic O cannot do the same to preadsorbed H. It is not known whether this result is specific to the C(111) surface, since both theoretical and experimental studies have shown that the adsorption of O proceed more readily on the prehydrogenated H:C (100) 2 × 1 than on the clean surface.[16,17] The recent X-ray scattering study of the C(111) surface following high-pressure oxygen−water oxidative etching by Theije et al. suggested that the surface was terminated by a full monolayer of OH instead of carbonyl or ether species.[14]

To provide insights into the H−O exchange on diamond (111) surface, we carry out TPD and UPS on diamond (111) in this work. We focus our investigation on the interactive exchange of O with chemisorbed D, and vice versa on diamond (111) and search for possible desorption products such as hydroxyl and water besides CO and CO_2. The characteristic valence band structure of diamond after interaction with atomic oxygen species was recorded. In addition, various configurations for O chemisorption on C(111) were considered using periodic density functional theory and the oxidation and hydroxylation processes simulated in terms of its reaction heat in order to provide a molecular basis for explaining our experimental results.

2. Experimental Section

2.1. UPS and TPD Experiments. Surface science studies were carried out in a UHV chamber ($P \sim 1 \times 10^{-10}$ Torr) equipped with a concentric hemispherical analyzer for performing UPS and AES, reflection high energy electron diffraction (RHEED) for surface structural analysis, and a remote-discharged RF atom beam source for sample cleaning. The sample used was a boron-doped semiconducting diamond thin film grown homoepitaxially on 6 mm × 6 mm synthetic (111)-oriented diamond substrate using microwave plasma enhanced chemical vapor deposition. For the UPS study, atomic O or H generated from a 13.56 MHz RF plasma beam source was used to irradiate the sample face. TPD was performed with a differentially pumped (400 L/s), shrouded quadrupole mass spectrometer with line-of-sight of the sample face. The multiple ion monitoring mode was used to monitor for various desorbing species during TPD. The diamond sample was heated by a 0.3 mm thick tantalum backing foil sandwiched tightly between the diamond and an insulating sapphire crystal. The tantalum foil could be heated resistively by proportional integrating differentiating (PID) temperature feedback control with a thermocouple buried at the back face of the diamond. A linear heating rate of 7 K/s was applied between 25 and 1200 °C during the TPD. The crystalline integrity of the diamond sample during multiple adsorption/desorption cycles was checked by monitoring the Auger C KVV fine features and the electron energy loss features associated with graphite shake-up satellite ($\pi \rightarrow p^*$).[27] The diamond sample could be cleaned by exposure to hydrogen plasma treatment generated from a RF-discharge at a substrate temperature of 800 °C if signs of surface graphitization were detected.

2.2. Periodic DFT Calculations of Oxidized Diamond Face. The total-energy calculations and optimizations were performed for all the considered oxygen, hydrogen, and hydroxyl chemisorbed C(111) systems using the plane-wave pseudopotential method (CASTEP) on the basis of density-functional theory in the local density approximation (LDA) for exchange and correlation.[18] The Vanderbilt ultrasoft pseudopotentials were used.[19,20] The wave functions were expanded into plane waves up to an energy cutoff of 680.25 eV. Special k points generated according to Monkhorst−Pack scheme[21] were used for integration over the irreducible wedge of the Brillouin zone for the various surface structures. The geometry optimizations were performed by the Broyden−Fletcher−Goldfarb−Shanno (BFGS) routine.[22] The exchange and correlation energies were calculated with the Perdew−Wang form of the generalized-gradient approximation (GGA).[23] The equilibrium lattice constant of 3.553 Å was obtained by optimizing the unit cell of bulk diamond. This value represents the experimental data of 3.567 Å with an error of less than 0.4%. We used this lattice constant for all further surface computations.

The supercell method was used to calculate the diamond surface systems and molecular systems, where the crystal surface is represented by a thick slab (12 carbon layers) with vacuum region (10 Å) and a molecule (such as O_2, H_2, H_2O) was put in a large cubic box with cell parameter of 10 Å. The spin-polarization energy was included for total energy of free atoms. The bottom of the slabs was saturated by H. The thickness of slabs and vacuum region had been tested to be large enough to avoid the interaction between the replicas.

The reaction heat is defined as follows:

$$\Delta E = \sum E_{(\text{product})} - \sum E_{(\text{reactant})}$$

where ΔE is the reaction heat and $E_{(\text{product})}$ and $E_{(\text{reactant})}$ are the total energy of each product and reactant, respectively. The total energies of O_2, O, H, and H_2O molecules at their equilibrium geometries were calculated to evaluate the reaction heats. It must be pointed out that our calculations were done at 0 K and did not take into account temperature effect and zero-point energy, thus the calculated reaction heats may be systematically overestimated (i.e., more exothermic).[16]

3. Results and Discussion

3.1. UPS and RHEED. Figure 1a shows the RHEED image of the as-grown C(111) surface, revealing a streaky 1 × 1 pattern coexisting with transmission spots, due to the presence of both microfacets and smooth domains on the surface. The grazing angle and long probing length of RHEED renders the technique especially sensitive to surface roughness due to microfaceting, the latter aspect is difficult to avoid for homoepitaxy on C(111) substrate that has dimension in the range of 6 × 6 mm. After annealing to 800 °C, a 1 × 1 to 2 × 1 transition occurs, as evidenced by the appearance of half-order fractional streaks between the integer order streaks in Figure 1b. The 2 × 1 reconstruction is characteristic of the π-bonded Pandey chain structure adopted by the hydrogen-free surface.[24] The occurrence of the 2 × 1 indicates that the smooth domains on the CVD diamond (111) surface are sufficiently well-ordered to undergo reconstruction.

The first series of experiments studied the kinetics of oxygen uptake by the clean diamond surface using Auger electron spectroscopy. We have applied Optical Emission Spectroscopy to monitor for the presence of O_2^+ or O* species in our RF-plasma discharge. Spectral lines due exclusively to the I lines of excited atomic O at 777.2 (strongest), 645.5, 615.8, 543.6, 532.9, 436.8, and 394.7 nm were detected, while no O_2^+ spectral lines (559.8 nm) was observed, testifying that the atomic beam source produced predominantly atomic O (excited and ground-state species). Two phases in the uptake of O can be discerned from the uptake curve in Figure 2. A few representative wide scan Auger spectra for the C and O auger signals are shown on

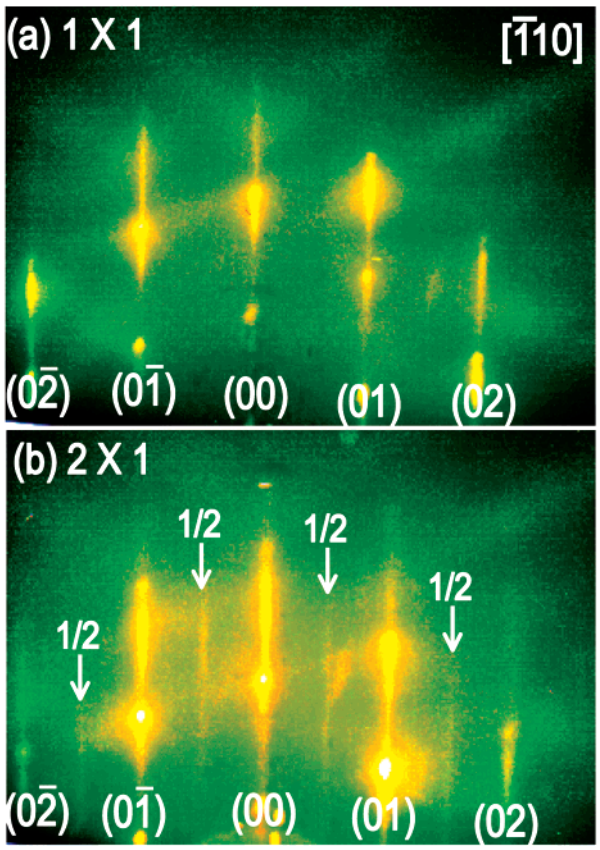

Figure 1. RHEED image showing the (a) as-grown C(111) 1 × 1 surface and (b) C(111) 2 × 1 reconstruction after annealing the surface to 900 °C in a vacuum.

the right-hand side of Figure 2. The O coverage was estimated from the overlayer attenuation formula using respective atomic sensitivity factors and mean free paths of carbon and oxygen atoms.[35] The O intensity saturates rapidly at room temperature to attain about 0.5 ML coverage after 5.4 × 10^5 Langmuir of doses. Further increase in coverage occurs only when the substrate temperature was raised to 400 °C during the treatment. For low-temperature oxidation, the 2 × 1 fractional streaks that is characteristic of the reconstructed face can still be seen, albeit weaker in intensity. A 2 × 1 to 1 × 1 transition occurs when the substrate temperature was increased to 400 °C to induce a further uptake of O on the surface.

Figure 3a shows the UPS He (I) spectrum of C(111) that has been subjected to H-plasma treatment. A sharp secondary electron peak characteristic of final state emission from a negative electron affinity (NEA) surface can be seen at the high binding energy end (low kinetic energy).[25,26] The changes in the intensity of this NEA peak was found to be a sensitive function of the surface work function changes arising from O−H exchange on the surface. The uptake of O on the hydrogenated C(111) was investigated by exposing it to O-atom beam treatment at room temperatures for different indicated times until the spectral features remain constant. It can be seen that the sharp secondary electron peak is totally attenuated after just 3 min of O atomic beam treatment (1.8 × 10^5 Langmuirs) in Figure 3b. The low kinetic energy cutoff is shifted to 14 eV, where its kinetic energy position is now larger than the band gap, as is characteristic of a positive electron affinity surface. In addition, strong O-induced valence emission states, highlighted in the difference spectra in Figure 3c, can be seen. These features centered at ∼4 and 8.5 eV can be assigned to O 2p surface states, and gain in intensity with increasing O atom beam treatment time. The valence band structure of the oxygenated diamond has a characteristically narrow spectral width compared to the hydrogenated surface.

Annealing the oxygenated C(111) to increasingly high temperatures resulted in the attenuation of O 2p-related features as shown in the UPS spectra in Figure 4. The low energy cutoff shifted to increasingly lower kinetic energies, indicating a reduction in surface work function with O desorption. By 400 °C, the pronounced O-related emission state at 4 eV has attenuated even though no recovery of the sharp NEA peak is achieved at this point, suggesting that the surface chemisorbed H has been exchanged dynamically during the O dosing. A roughly ±1.5 eV shift in the low kinetic energy cutoff was attained upon annealing to 900 °C, where Auger analysis

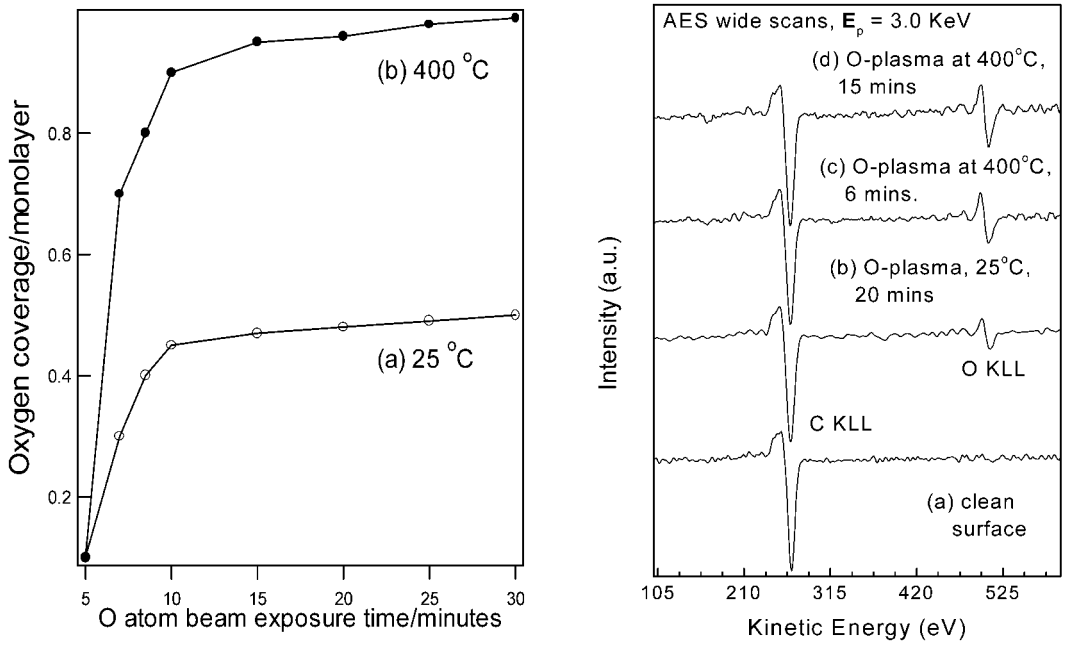

Figure 2. AES uptake curve for oxygen, monitoring the uptake of O on the surface (a) at room temperature; which saturates near 50% coverage and (b) at 400 °C, where full O coverage can be attained. The figure on the left shows selected wide scan spectra.

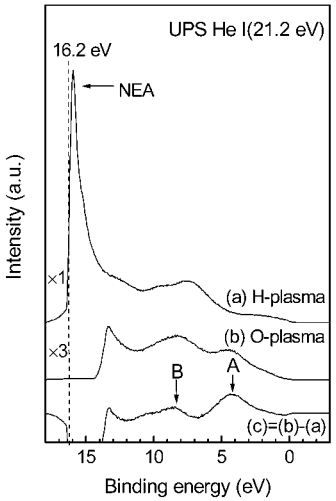

Figure 3. UPS He(I) spectra showing changes in the valence band features during the uptake of O on the surface. Note the attenuation of the NEA peak and the occurrence of O *2*p-related surface states highlighted in the difference spectra.

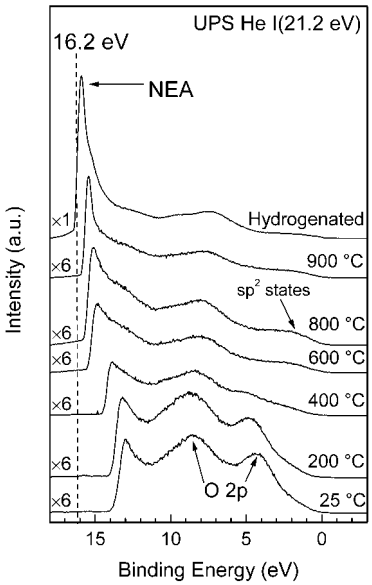

Figure 4. UPS He(I) spectra showing changes in the valence band features following the annealing of the surface to successively higher temperatures.

indicated that O was completely desorbed from the surface at this point. A small increase in emission intensity near the Fermi level which is characteristic of *defect or* sp^2 *states* is also observed in the UPS spectrum at this point. This intensity increase is accompanied by changes in the fine-structure of the carbon *KVV* Auger carbon peak, as shown in Figure 5. For example, peak A_3 has gained in intensity relative to A_1 in the positive excursion of the C *KVV* Auger.[27] These changes suggest that the C(111) surface has graphitized following the desorption of O from the surface. It is noteworthy that the C(111) surface is readily graphitized after post-oxygen plasma treatment annealing. The graphitized C(111) has to be subjected to a second hydrogen-plasma treatment to recover the sp^3 integrity, the changes in the Auger fine features are depicted in Figure 5d,e.

The uptake of hydrogen on the oxygenated C(111) surface is investigated by exposing the oxygenated surface to atomic H beam irradiation. Figure 6 shows the changes in the spectral features at interrupted intervals. The estimated upper flux of atomic hydrogen is about 100 monolayers/s based on a previous uptake curve calibrated by elastic recoil detection analysis.[36]

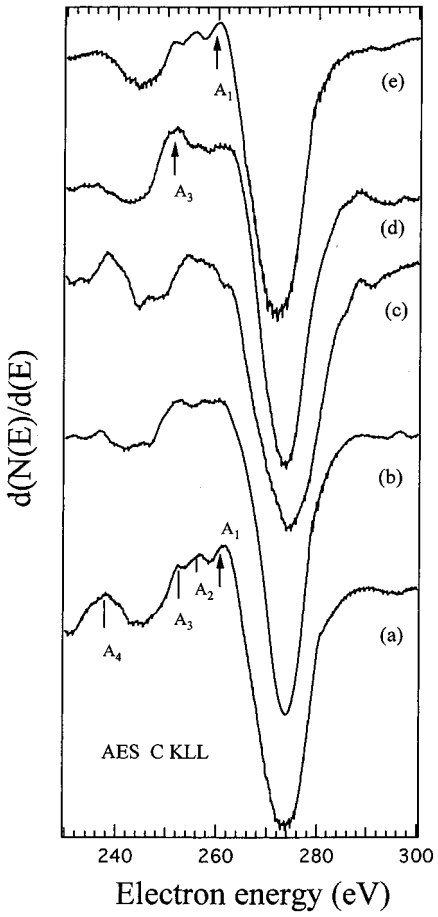

Figure 5. High-resolution Auger showing (a) RF hydrogen-plasma treated C(111), (b) oxygen beam-treated at room temperature, (c) oxygen beam treated at 400 °C, (d) annealed to 1000 °C, and (e) retreated with RF hydrogen-plasma.

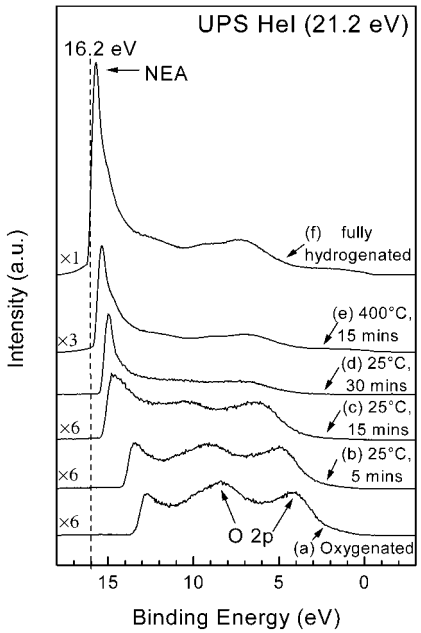

Figure 6. UPS spectra of C(111) surfaces obtained after (a) O-plasma treatment and subsequent H-plasma exposure at 25 °C for (b) 3×10^5 L, (c) 9×10^5 L, (d) 1×10^4 L, and at (e) 400 °C for 9×10^5 L, respectively (L = Langmuir = 1×10^{-6} Torr. s). The spectrum of fully hydrogenated surfaces is shown as spectrum f.

From the slow change in the spectral feature of the oxygenated C(111) between room temperature to 400 °C, it can be seen

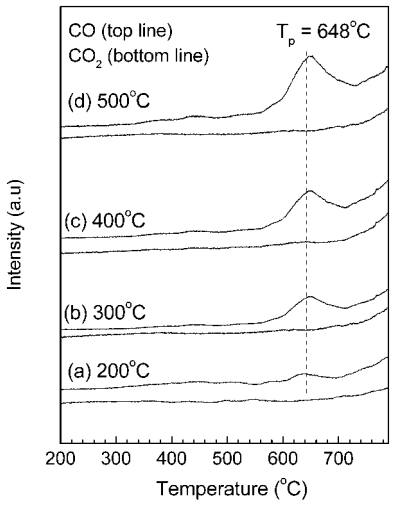

Figure 7. TPD signal tuned to CO ($m/e = 28$ amu) for clean C(111) surface exposed to O plasma beam at different temperatures. A fixed O dose of 3×10^5 L was applied on the different samples.

that the exchange process of chemisorbed O by atomic H is not very efficient at low temperature. On the bases of the H exposures needed to cause the O signal to disappear, an apparent reaction probability of 1×10^{-6} for the H−O exchange is derived. With increasing time of H irradiation, we can see that the O *2*p features are suppressed, along with the extension of the spectral width and corresponding reduction in the kinetic energy of the low energy cutoff. But no complete recovery of the initial NEA condition characteristic of the fully hydrogenated surface could be obtained even after prolonged exposure to H atom beam at room temperature. Some oxygen species remain bound on the surface, possibly at defect sites, where they resist removal at room temperature. Finally, increasing the substrate temperatures to 400 °C during the atomic H beam treatment facilitates the complete removal of oxygen from the surface.

3.2. TPD. In the first series of TPD experiments, the atomic O beam treatment was performed on the clean C(111) substrate with the substrate annealed at a constant temperature in order to investigate the effect of thermal activation on oxygen uptake. A fixed O dose of 3×10^5 Langmuirs was irradiated on the samples. The substrate was then allowed to cool to room temperature before a TPD scan was performed. The TPD plots recorded for different substrate temperatures during the O-dosing were stacked in Figure 7. The desorption signals of CO ($m/e =$ 28 amu) and CO_2 ($m/e = 44$ amu) were monitored. A desorption peak centered at 650 °C was found to increase with the substrate temperature during the O atom beam treatment. No signal corresponding to CO_2 was detected. No shift in the peak desorption temperature was seen with surface coverage, indicating first-order desorption rate kinetics. From Redhead's[28] analysis of first-order desorption kinetics, the peak desorption rate temperature corresponds to an activation energy for CO of 59 kcal/mol, if a prefactor of 10^{13} s^{-1} is assumed. A simple explanation for the absence of CO_2 desorption suggests that the majority of the bonding states for oxygen on C(111) originate from a carbon atom bonded to a single oxygen atom or fewer, as in the bonding stoichiometric CO or C_2O. The increase in CO desorption yield with substrate temperature could be a consequence of two factors: (i) the increased roughening of the surface at higher oxidation temperature, resulting in a higher density of defect sites and facets with larger surface area for O chemisorption; (ii) a change in O chemisorption state at higher temperatures. The change in O chemisorption states with different O coverage on the surface is shown in the DFT calculations in section 3.3.

To investigate the coadsorption behavior of O and D on the surface, a preoxygenated surface was exposed to atomic D at 400 °C. TPD peaks were then scanned for OD, D_2O, D_2, CO, and CO_2. Figure 8a shows the TPD signal recorded for D_2, showing an increase in the desorption yield with longer exposure times to atomic D. Corresponding desorption signals for CO in Figure 8b shows a decay in yield. This means that the surface O is depleted with exposure to atomic D, indicating a D−O exchange. Possible products such as OD and D_2O that arise

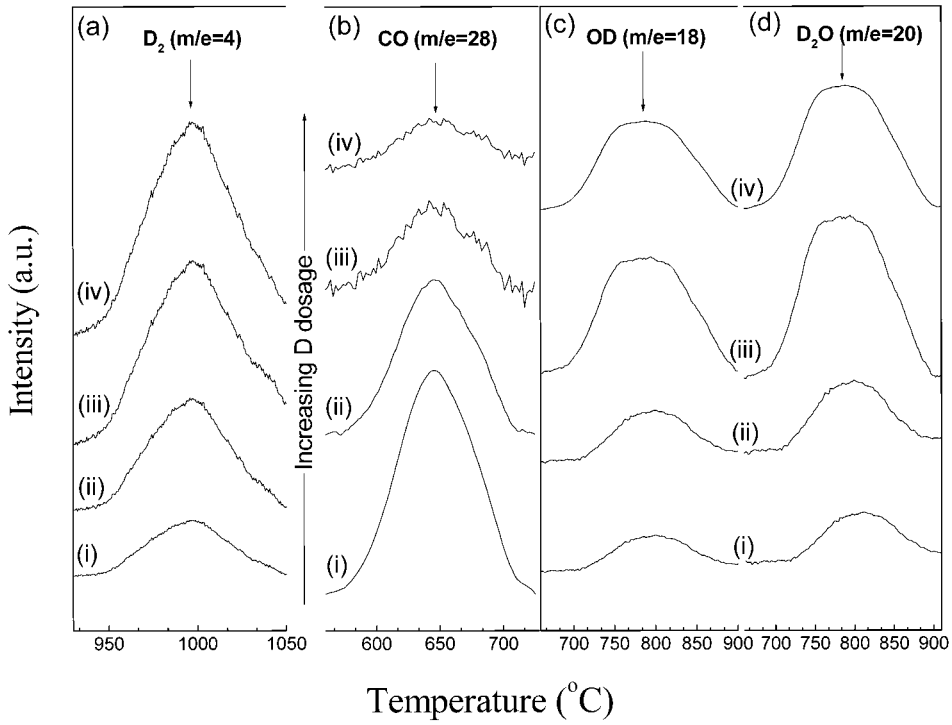

Figure 8. TPD tuned to (a) D_2 ($m/e = 4$ amu), (b) CO ($m/e = 28$ amu), (c) D_2O ($m/e = 20$ amu), and (d) OD ($m/e = 18$ amu) for a pre-oxygenated C(111) surface that was exposed to atomic D at 400 °C for (i) 9×10^4 L, (ii) 1.8×10^5 L, (iii) 3×10^5 L, and (iv) 4.8×10^5 L, respectively.

TABLE 1: The Various Structural Parameters (in Ångstroms) and the Chemisorption Energies for Oxygen Chemisorption on C(111) Surfaces

systems	d_{o-c}	d_{o-o}	d_{c-c}	chemisorption energy/eV	remarks
1 × 1 on-top H				4.89	
1 × 1 on-top O	1.326			4.24	Figure 10
1 × 1-peroxy O	1.432	1.565		4.85	Figure 11
1 × 1 on-top OH	1.435			4.34	Figure 13
2 × 1: 2H			1.555, 1.561	4.44	Figure 18
2 × 1: epoxy O	1.433		1.457 (with O in bridge) 1.498 (without O in bridge)	5.23	50 % O coverage, Figure 19
2 × 1: carbonyl O	1.195	2.617, 2.480	1.703, 2.318	4.85	full O coverage, Figure 20
2 × 1: OH, H	1.448		1.561, 1.563	4.16	50 % OH coverage, Figure 14
2 × 1: OH, OH	1.407		1.579	3.99	Figure 16

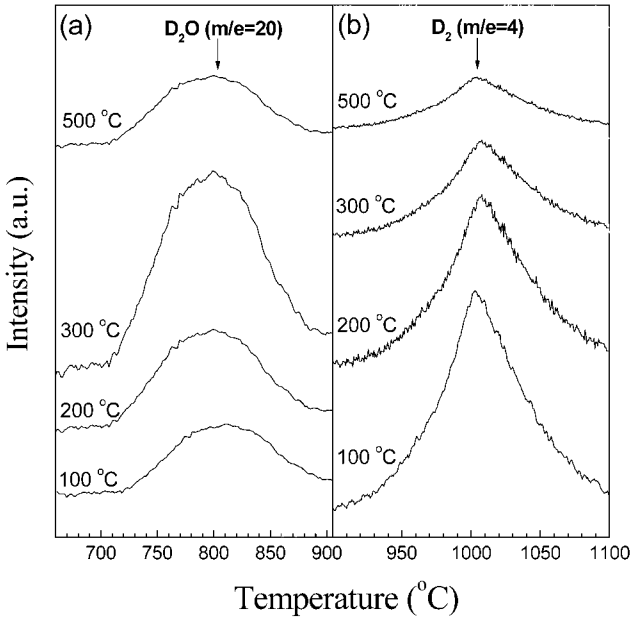

Figure 9. TPD signal tuned to (a) D_2 (m/e = 4 amu) and (b) D_2O (m/e = 20 amu) for a pre-deuterated C(111) surface that was exposed to atomic O at increasingly elevated temperatures. A fixed O dose of 3×10^5 L was applied on the samples.

from the chemistry between O and D were also monitored. Figure 8c shows the increasing yield of OD and D_2O near 800 °C. The signal of OD is assigned to the mass spectrometer-induced cracking fragments of D_2O.

The exchange of atomic O with D on predeuterated C(111) surface at different temperatures was also investigated by TPD. Parts a and b of Figure 9 show an increase in the desorption yield of D_2O (m/e = 20 amu) and D_2 (m/e = 4 amu) that was observed with increasing substrate temperature during exposure to atomic O, suggesting a thermally activated process that might originate from the insertion of O into C−D bonds to form C−OD, and their subsequent recombinative desorption with D to form D_2O. At 500 °C, there is a drop in the yield of D_2O and D_2, this may be due to the reduced coverage of D on the surface following the more efficient exchange. Figure 9b indicates a clear decline in the surface coverage of D with exposure to atomic O. The relative intensity of OD:D_2O of 0.27:1 agrees with the mass spectrometer-induced cracking fragments of D_2O, so only D_2O, D_2, and CO were the actual desorption products.

3.3. Periodic DFT Calculations. The various structural parameters (in angstroms) and the chemisorpton energies for oxygen chemisorption on the C(111) surfaces are listed in Table 1. Several of these structures have quite similar chemisorption energies, suggesting that these systems may coexist.

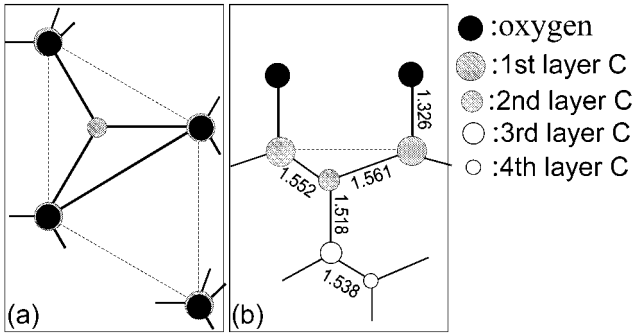

Figure 10. Optimized structure of on-top oxygen on bulk truncated C(111) surface: (a) top view and (b) side view. Length unit in angstrom. Only the first two layers of atoms are shown.

(*A*) *Oxygen on C(111) 1 × 1.* We begin by examining several models for atomic oxygen chemisorption on the single dangling bond C(111) surface. Three different bridged sites on the bulk-terminated surface were considered. As the optimization step continues however, the O atoms in the bridged site will move toward the on-top site shown in Figure 10, suggesting that the on-top site for the 1 × 1 surface is the local energy minima. The C−O bond lengths were determined to be 1.326 Å with a chemisorption energy of 4.24 eV per surface O. This chemisorption energy is lower than that of hydrogen termination of the single dangling bond (4.89 eV). The termination of single bond surface by O atom alone is not likely considering the dangling bond on O atom. Termination by OH appears to be more likely considering the ubiquitous presence of hydrogen and the affinity of the lone pair electron on O to bind to H.

Another possible alternative involves the binding of molecular oxygen in a peroxy fashion spanning two carbon sites and parallel to the surface, as shown in Figure 11. This binding mode has been suggested for low-temperature adsorption of oxygen and has been attributed to one of the vibrational stretches (657 cm^{-1}) observed by a recent multiple internal reflection infrared spectroscopy study.[12] Alternative bridged site in the [01$\bar{1}$] or [10$\bar{1}$] direction has a peroxy oxygen species spanning it. The chemisorption energy of this configuration relative to the bare surface is determined to be 4.85 eV per oxygen atom with a O−O bond length of 1.565 Å and a C−O bond length of 1.417 Å. Such a peroxy bridged site model has been considered previously by Zheng et al. using SLAB-MINDO calculations where they obtained a O−O bond length of 1.49 Å and a C−O bond length of 1.43 Å.[29] The reaction heats of formation of this structure from the reaction of single dangling bond C(111) 1 × 1 surface with molecular O_2 is calculated to be exothermic

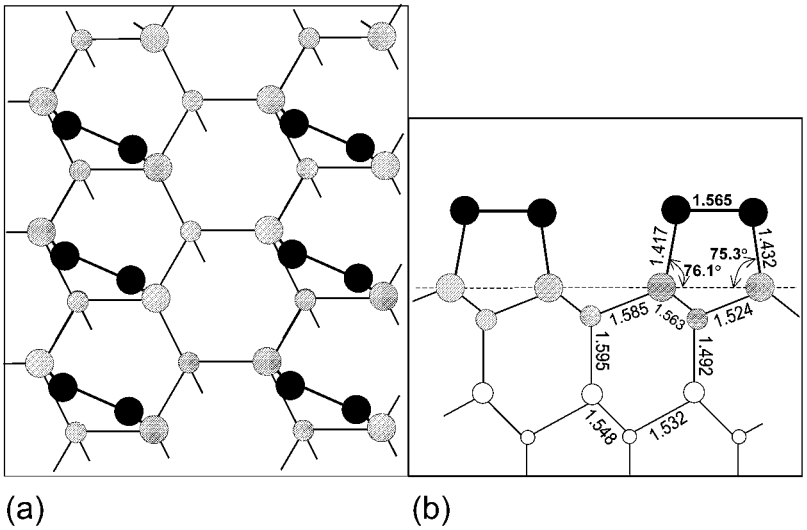

Figure 11. Optimized geometry of the oxygen peroxy species on bulk truncated C(111) surface: (a) top view and (b) side view. Length unit in angstrom.

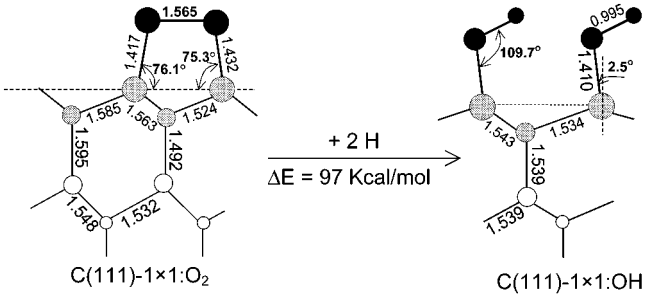

Figure 12. Conversion of peroxy C(111)-1 × 1:O_2 to hydroxyl C(111)-1 × 1:OH by interaction with atomic H.

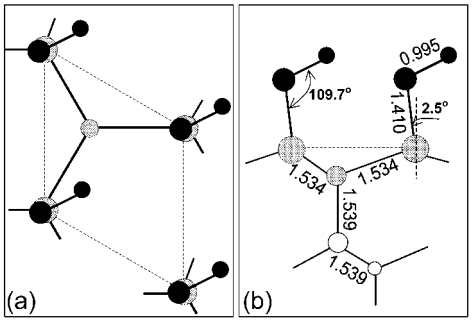

Figure 13. Optimized geometry of the hydroxyl groups on bulk truncated diamond (111) surfaces: (a) top view and (b) side view. Length unit in angstrom. The small and big bold circles represent H and O atoms, respectively.

by 90 kcal/mol in this study. However due to the weak CO−OC bond compared to the CO−H bond [38 versus 105 kcal/mol], the peroxy structure will more likely convert into −OH in the presence of H, as shown in the schematic in Figure 12. An exothermic reaction heat of 97 kcal/mol is calculated for the hydroxylation of the peroxy structure.

(*B*) *The Formation of Hydroxyl Groups.* The formation of hydroxyl terminating group on C(111) 1 × 1 surface is considered. The side view and top view of the optimized best-fit model of the OH-terminated surface is shown in Figure 13. The C−O−H bond is tilted at an angle of 109.7 and the C−OH bond length is 1.410 Å, with a chemisorption energy of 4.34 eV per OH group. A slight tilt of the C−OH bond by 2.5° is found, due possibly to the minimization of steric repulsion among the OH groups. Theije et al.[14] has determined the atomic structure of the {111} diamond face after oxygen−water vapor

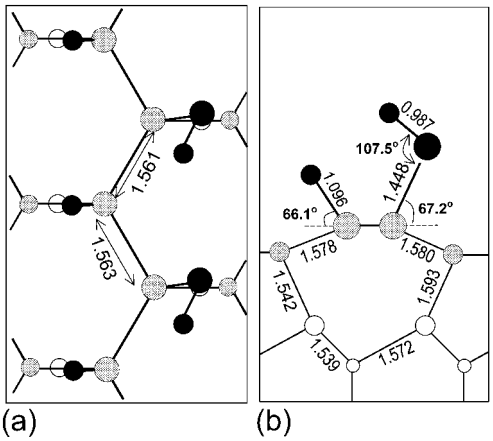

Figure 14. Optimized structure of chemisorbed OH and H on C(111) 2 × 1 surfaces: (a) top view and (b) side view.

etching using X-ray scattering and found that a single dangling bond surface terminated by −OH best fits the data. The hydroxyl group can be generated by exposing either the oxygen-terminated O:C(111) 1 × 1 surface to atomic hydrogen, or by exposing the hydrogenated H:C(111) 1 × 1 to atomic oxygen. The exothermic reaction heat of formation of the C(111)-1 × 1 monohydride face to form OH:C(111)-1 × 1 from atomic O is calculated to be 191 kcal/mol, while the reaction heat from the corresponding O:C(111)-1 × 1 and atomic H is 224 kcal/mol.

For the adsorption of hydroxyl groups on the C(111) 2 × 1 surface, a possible model is the binding of the OH and H species on alternate carbon dimer in the Pandey chain, indicated in Figure 14. This structure may be an intermediate that forms after (i) the epoxy O on the C(111) 2 × 1 is attacked by atomic H and (ii) the hydrogenated C(111) 2 × 1 suffers an O insertion into one of the C−H bond. The various pathways that will lead to the hydroxyl-terminated OH:C(111) 1 × 1 is shown in Figure 15. The optimized C−OH bond and O−H bond distances are calculated to be 1.448 and 0.987 Å respectively, with a ∠C−OH bond angle of 107.5°. Interestingly, the carbon in the Pandey chains are now slightly buckled and the C−C bond distances have been modified to 1.563 Å and 1.561 Å alternatively, which are closer to the bulk C−C bond distances. To maintain the 2 × 1 structure for a full OH termination of the adjacent dimer carbon, a staggered configuration of the OH group is necessary

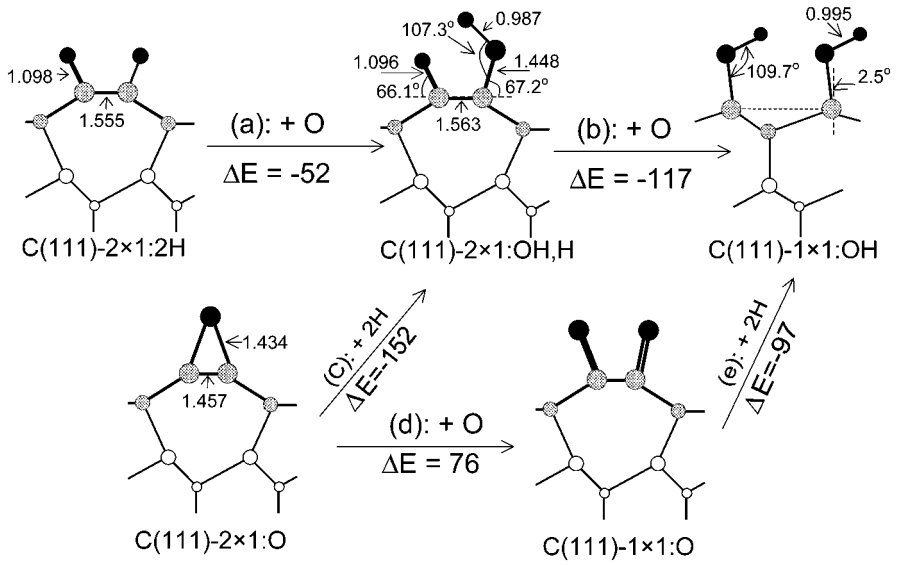

Figure 15. Reaction pathways to form the final stable product C(111)-1 × 1:OH.

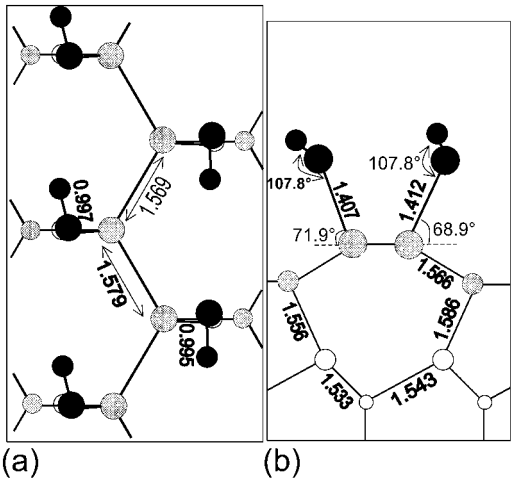

Figure 16. Optimized structure of full OH termination on the C(111) 2 × 1 surfaces: (a) top view and (b) side view.

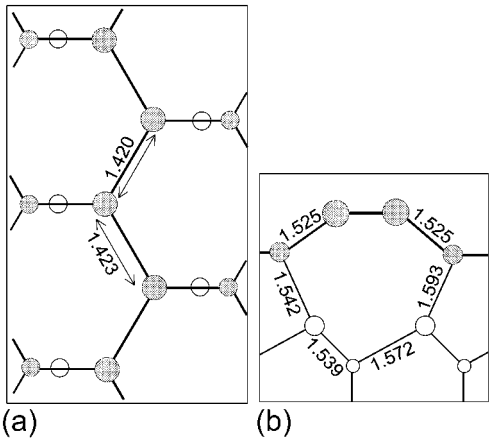

Figure 17. Optimized geometry of reconstructed C(111) 2 × 1 surface: (a) top view and (b) side view.

to prevent steric repulsion of the OH groups, as shown in Figure 16. The chemisorption energy per OH group of 3.99 eV is the lowest among all the systems considered here however, and at elevated temperatures, this metastable structure will most likely convert to the bulk-terminated 1 × 1-hydroxyl surface.

The exothermic reactions heat of formation of the O:C(111)-2 × 1 surface with atomic H to form OH,H:C(111)-2 × 1 (structure as shown in Figure 14) is calculated to be 152 kcal/mol (per C(111)- 2 × 1 unit cell). If the starting reactant is the 2H:C(111)-2 × 1 structure and atomic O, the exothermic heats of reaction is 52 kcal/mol (per C(111)- 2 × 1 unit cell). The different pathways are illustrated in Figure 15a,b. The exothermic heats of reaction suggest that the formation of hydroxyl species from the hydrogenated or oxygenated C(111) surface when exposed to atomic O or atomic H will be favored thermodynamically, and that the coadsorption of hydroxyl species with chemisorbed H or O on the diamond surfaces can yield stable structure. This is contrasted with the relatively smaller exothermic heat of reactions from the reaction between the clean diamond 2 × 1 surface and water (calculated to be 8.3 kcal/mol) to give OH,H:C(111)-2 × 1 suggesting that a thermodynamically feasible pathway of generating hydroxyl groups on the surface is to proceed via the oxygenated or hydrogenated C(111) surface instead of the clean surface. It must be pointed out however that activation energies needed to form the considered structure may exist and is not reflected in our methods of calculations.

(*C*) *2 × 1 Configuration and Monohydrogenated C*(*111*):*H Surface.* The associative desorption of hydrogen from the hydrogen-terminated (111) single dangling bond surface to generate the clean C(111) 2 × 1 surface, as calculated in this study, is endothermic by about 120 kcal/mol. The optimization of the reconstructed C(111)−(2 × 1) surface was started from the ideal geometry proposed by Pandey.[24] The optimized C−C bond distance is $d = 1.420$ Å and the alternative C−C bond is 1.423 Å, as shown in Figure 17a,b. Adsorption of a monolayer of atomic hydrogen on the reconstructed C(111)-2 × 1 surface results in a gain in chemisorption energy of 4.44 eV relative to the bare surface. The bond length in this chain now is modified from the value of 1.420 Å to 1.555 Å. Figure 18 shows the H:C(111) 2 × 1 surfaces. The bond length of C−H is 1.099 Å. These values agree very well with the ab-intio LDF methods of G. Kern et al.[30] who found that the C(111) 2 × 1 Pandey chain remains stable after adsorption of a monolayer of hydrogen, only that the C−C bond length now is increased to 1.55 Å, i.e., almost identical to the bulk value. This means that the saturation of two of the dangling bonds breaks the π bond and allows for the formation of surface dimers in analogy to the monohydride C(100) 2 × 1 surface. Recent infrared sum−frequency generation experiments detected additional peak at

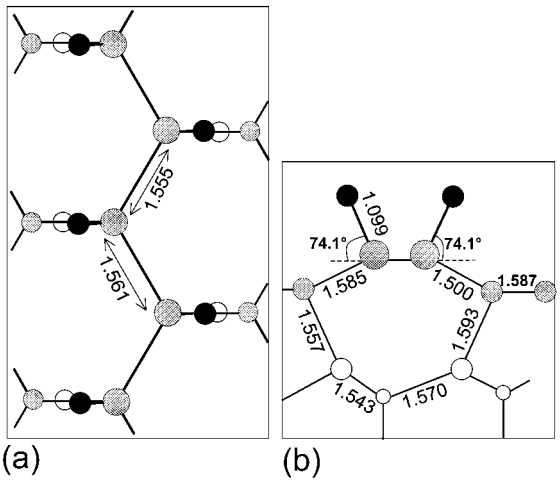

Figure 18. Optimized geometry of reconstructed H:C(111) 2 × 1 surface: (a) top view and (b) side view.

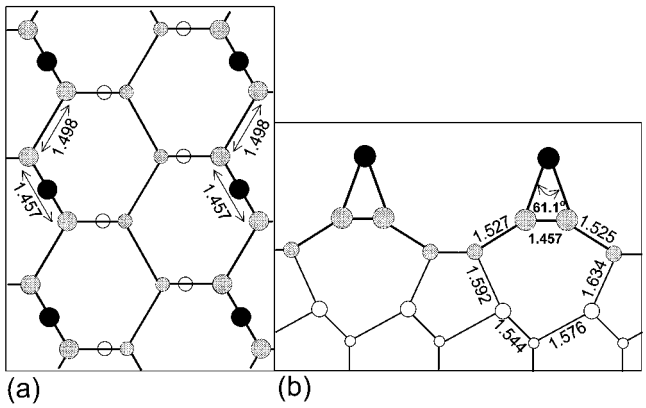

Figure 19. Optimized geometry of half-monolayer epoxy oxygen on C(111) 2 × 1 surface: (a) top view and (b) side view.

low H coverages that may arise from the metastable hydrogenated C(111) 2 × 1 structure before its conversion into the C(111) 1 × 1.[31,32] We consider the possibility of inserting an oxygen atom in a bridging fashion between the two hydrogenated carbon in the Pandey chain. However after optimization, it was found that the O has moved and inserted into the C−H bond to form C−OH instead, giving rise to the structure shown in Figure 14. The C−C stride of 1.56 Å in H:C(111) 2 × 1 surface is far too short for O insertion due to steric repulsion from the two neighboring H, this is unlike the case of the coadsorbed O which forms an ether-like bridge structure in C(100) 2 × 1 monohydride.[16]

(*D*) *O:C(111) 2 × 1 Surface.* The minimum-energy configuration for half-monolayer atomic O chemisorption on the alternate bridged site of the π-bonded chain on the clean C(111) 2 × 1 surface is shown in Figure 19. For a hydrogen-free surface, the O atom can bind in an "epoxy" mode between alternative C−C in the zigzag chain without lifting the 2 × 1 reconstruction. Because the equilibrium C−C distance stride across the O atom of this structure is very short (1.457 Å), the COC angle is constrained to 61.1° and is markedly different to the COC angle found in free ether or that of the etherized structure in oxygenated C(100) 1 × 1.[16]

The formation of this epoxy structure from the clean C(111) 2 × 1 surface and atomic oxygen is exothermic by 86 kcal/mol. A chemisorption energy of 5.23 eV and a C−O bond length of 1.434 Å with a COC bond angle of 61.1° is obtained. The zigzag carbon bond distances are now 1.457 Å and 1.498 Å with and without oxygen in the bridged site. The chemisorption

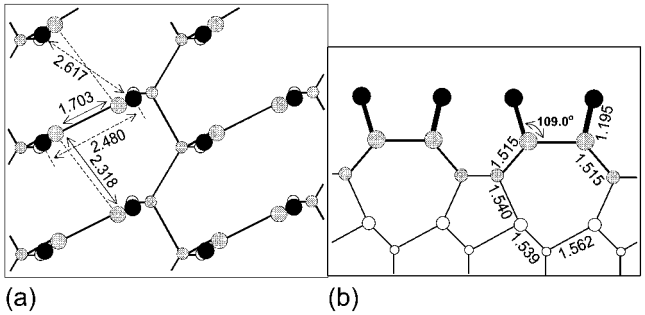

Figure 20. Optimized geometry of monolayer carbonyl oxygen on C(111) 2 × 1 surface: (a) top view and (b) side view.

energy for this system is the highest among all the adsorption systems studied in this work, indicating that this may be the preferred O binding structure, at least during the initial stage of O uptake.

For a full O coverage, O adsorbing in an "on-top" fashion on each carbon of the zigzag chain is considered. The initial Pandey chain of the clean 2 × 1 surface however is broken following the optimization process, as illustrated in the drawing in Figure 20a,b. We started the process by adsorbing an oxygen molecule in a peroxy-like fashion along the zigzag chain, after optimization, the O atoms move to the nearly "on-top" position of the carbon atoms along the chain with C−O bond length = 1.195 Å and the ∠OCC = 109.0°. The C−C bonds along the zigzag chain are now expanded to 1.703 and 2.318 Å, respectively, a clear evidence that the Pandey chain has been broken following full oxygen coverage. The chemisorption energy for this system is 4.85 eV compared to the bare surface. More importantly, the optimized C−O bond length for this configuration is now 1.195 Å, suggesting that the bonding is more akin to a carbonyl-type species in acetone. Therefore our calculations predict that at the early stage of O adsorption on the clean C(111) surface, an epoxy-like C−O−C bonding will dominate up to 50% surface coverage. At higher O coverage, transition to a carbonyl-type C═O linkage will occur with a consequent lifting of the 2 × 1 reconstruction. The heat of reaction from the epoxy O bridging species to carbonyl-like, on-top O species is calculated to be exothermic by 76 kcal/mol, as shown in the scheme in Figure 15d. However, in the presence of atomic H, these C═O-topped C(111) surface adopting a zigzag configuration is readily converted to OH-terminated bulk-terminated C(111) 1 × 1 surface as shown in Figure 15e. An exothermic reaction heat of 97 kcal/mol is calculated.

Discussion

This study provides some insights into the mechanism of oxygen adsorption and desorption in association with its binding configuration on the C(111) surface. The UPS study reveals that distinct O-induced surface states can be seen in the valence band spectrum at room temperature after the exposure of a hydrogenated C(111) 1 × 1 surface to atomic O, which evidences that the uptake of O is facile on the hydrogenated surface. The lack of a probe sensitive to vibrational stretches prevent us from confirming whether the chemisorbed O is existing as C−O, C−O−C, or C−OH species. From changes in the UPS spectra, it is clear that the effect of O chemisorption is to change the surface into a positive electron affnity condition. The recovery of the NEA state is not possible even with the subsequent desorption of O from the surface, indicating that a dynamic O−H exchange has taken place to deplete the surface H population which is responsible for the NEA. The subsequent

desorption of O from the surface results in the appearance of features associated with defects. In another series of study, it was shown that chemisorbed O could be removed from the surface by exposure to atomic H, except that the process appeared to be relatively inefficient at room temperature in high vacuum conditions because O *2*p-related surface states survive for a long time during such treatments. One possibility is that the O is converted to *stable hydroxyl groups* by atomic H, and these species have no efficient escape route from the surface at room temperature.

Among all the chemisorption sites considered in this study for oxygen adsorption on C(111) 1 × 1 and 2 × 1, all have the carbon atoms bonded to single O species. The configuration of the single dangling bond C(111) face does not allow the existence of twin bonded species such as the ether structure (O−C−O) which has been previously detected by vibrational spectroscopy on the C(100) 2 × 1 surfaces.[9−11] This explains why only CO, and not CO_2, was observed as the desorption product on the C(111) face, in contrast to the C(100) face where CO_2 was detected in addition to CO.[8] Recently, B. L. Mackey performed TPD study on (110)-oriented diamond and observed both CO and CO_2 evolution.[12] Therefore the observation of only CO desorption from C(111) is unique among the three low index faces of diamond. The desorption of CO is equivalent to the etching of diamond because of the removal of carbon. The threshold for CO desorption on C(111) is 600 °C, suggesting that etching of diamond surface will proceed from this temperature onward.

It is instructive to ask this question: What is the configuration of a full monolayer O coverage on the C(111) 2 × 1 surface? Our experimental study show that at low oxidation temperature, uptake of the O on C(111) 2 × 1 surface can proceed without lifting the 2 × 1 reconstruction. Our DFT calculations reveal that the optimized oxygenated 2 × 1 structure has an epoxy oxygen spanning two carbon atoms of the Pandey chain (Figure 19), while the neighbor carbon dimer in the chain is not bonded to O. In such a case, the surface O coverage attained is only 50%. Our observation of a stable 2 × 1 reconstruction following oxygen adsorption at low temperature supports the previous observation of Klauser et al.[13] and lends support to the epoxy oxygen binding mode. In the subsequent desorption process between 600 and 800 °C, only 50% of the surface carbon will be removed as CO (since only one-half of the carbon in the chain will be removed), while the remaining 50% will become isolated surface carbon with dangling bonds, which could aggregate on the surface at high temperature to form graphitic phases. The unique character of this half-monolayer O binding state on C(111) explains our observation that the C(111) surface is readily graphitized after O adsorption and desorption/etching processes.

Our calculations show that at higher oxygen coverage on the C(111), a possible intermediate structure consisting of a full-monolayer of bonded C═O with incommensurate reconstruction may exist, as shown by the structure illustrated in Figure 20. The consequence of accommodating a full monolayer O (every surface C bonded to O) is the lifting of the 2 × 1 reconstruction because the fully occupied C═O bonded surface necessitates the breaking of the Pandey chain to accommodate double bond formation between carbon and oxygen. This could be the reason oxygen uptake is thermally activated because activation barrier for lifting the 2 × 1 reconstruction has to be overcome. Both AES and TPD studies indicated that the surface O coverage increased with substrate temperature during the O-plasma beam treatment, and RHEED showed a conversion of the 2 × 1 into 1 × 1. If desorption of CO proceeds from this structure, a complete layer removal of the surface carbon as CO is now possible. Therefore our work suggests that a layer by layer etching of diamond could only be possible with the complete oxidation of the C(111) surface, attained by subjecting the C(111) sample to O-plasma treatment at 400 °C or above. A low-temperature oxidation and heating cycles may result in incomplete etching and graphitization of the surface.

Both the TPD and UPS results verify that the exchange of O with chemisorbed D, and vice versa, can proceed on the C(111) surface readily even at room temperature. These processes are thermally activated such that a higher rate of exchange occurs at elevated temperature. At intermediate stage of exchange, products of the reactions between O and D such as D_2O can be observed. Considerations of the heats of reaction suggest that an oxygenated surface is not stable in the presence of atomic D/H because it is converted to an OD-terminated surface. This was corroborated by the yield of D_2O (OD + D) from the surface coadsorbed with O and D in the TPD experiments shown in Figures 8 and 9. Likewise, oxygen insertion into the C−D bonds on predeuterated surface can generate C−OD, and D_2O was subsequently generated from coadsorbed OD and D during TPD. A reaction scheme for the O−D or D−O exchange on C(111) can be proposed thus: Atomic O can insert into the C−D bond to form OD, and atomic D can react with chemisorbed O to form OD. These OD species can desorb combinatively with a neighboring D to form D_2O, thus freeing the surface sites for further reaction with gaseous O or D. The insertion of O into C−D and the desorption of D_2O are reactions with activation barrier, which explains why the O−D or D−O exchange processes of C(111) are thermally activated as observed by our TPD studies, i.e., increasing desorption yield of exchanged products at higher temperature. Our results did not support the claim by R. Klauser[13] that O cannot exchange preadsorbed H on C(111) because our UPS and TPD results show that uptake of O is facile even at room temperature. It must be pointed out however that excited, vibrationally hot O* species were inevitably generated in the plasma source and these species may enjoy a higher efficiency in inserting into the C−D bonds to form C−OD compared to ground state O. Another possibility is that energetic O ions may abstract H directly from the substrate face. The relative efficiency of the O−D exchange and etching may depend on the population distribution of excited O radicals, ground-state O and O ions in the plasma source.

Reaction heats considerations suggest that a fully OH-terminated C(111) 1 × 1 surface is the final stable product from the different precursor oxygenated states (Figure 15). In our TPD studies, we observed that water, a reaction product between coadsorbed OD, D and O species, desorbed from 800 °C onward. This means that if the surface is saturated with OD species, the etching of diamond, which has its onset starting at 600 °C for the clean surface, will be inhibited until at least 800 °C. This is a direct experimental verification of the etching study of Chu et al.[33] who found that diamond was not etched by water until a higher temperature than that initiated by oxygen, and suggested that water is a good oxidation inhibitor at temperatures below 850 °C, due possibly to the formation of C−OH bonds.

Conclusion

We have investigated the interaction of atomic O and D with (111)-oriented diamond. Both UPS and TPD studies indicated that the exchange of O with preadsorbed D, or vice versa, could proceed on the C(111) surface readily. Uptake of O on C(111) surface produced distinct O-induced surface states at 4 and 8.5

eV in the valence band spectra and resulted in a positive electron affinity condition. On the O-dosed C(111) 2 × 1 surface, CO was observed as the only desorption product at 650 °C. TPD experiments revealed a higher surface coverage of O when the C(111) 2 × 1 surface was treated with atomic O at higher substrate temperature, suggesting a thermally activated chemisorption process. Desorption of CO from a partially oxygenated C(111) surface resulted in residual surface carbidic species. On a pre-deuterated surface that was exposed to atomic O, or on a preoxygenated surface exposed to atomic D, reaction products such as D_2O could be observed to desorb from the surface at 800 °C.

Periodic DFT calculations suggest that there is a change in the O chemisorption states depending on the O coverage on the surface. At low O coverage (less than 50%), an epoxy-like O adsorbs on the Pandey chain of the C(111) 2 × 1 by occupying alternating next-nearest neighbor sites, such that the bonding stoichiometry is C_2O. At higher coverages (up to 100%), a carbonyl-like O bonding mode (CO) is more stable and the 2 × 1 reconstruction is lifted, i.e., every neighboring carbon atom is terminated by on-top O. In the presence of atomic H, reaction heat considerations suggest that the oxygen-chemisorbed surface may convert to a more stable hydroxyl-terminated C(111) 1 × 1.

References and Notes

(1) Yoshimoto, M.; Furusawa, M.; Nakajima, N.; Takakura, M.; Hishitani, Y. *Diamond Relat. Mater*. **2001**, *10*, 295.

(2) Sakaguchi, I.; Gamo, M. N.; Loh, K. P.; Hishita, S.; Haneda, H.; Ando, T. *Appl. Phys. Lett*. **1998**, *73*, 2675.

(3) Tachiki, M.; Fukuda, T.; Sugata, K.; Seo, H.; Umezawa, H.; Kawarada, H. *Appl. Surf. Sci*. **2000**, *159-160*, 578.

(4) Gluche, P.; Aleksor, A.; Vescan, A.; Eberl, W.; Kohn, E. *IEEE Electron Dev. Letts*. **1997**, *18*, 547.

(5) Chen, C. L.; Chang, H. C.; Lin, J. C.; Song, K. J.; Wang, J. K. *Phys. Rev. Letts*. **1997**, *78*, 3713.

(6) Thoms, B. D.; Butler, J. E. *Surf. Sci*. **1995**, *328*, 291.

(7) Kuttel, O. M.; Diederich, L.; Schaller, E.; Carnal, O.; Schlapbach, L. *Surf. Sci*. **1995**, *337*, L812.

(8) Thomas, R. E.; Rudder, R. A.; Markunas, R. J. *J. Vac. Sci. Technol. A*. **1992**, *10*, 2451.

(9) Hossain, M. Z.; Kubo, T.; Aruga, T.; Takagi, N.; Tsuno, T.; Fujimori, N.; Nishijima, M. *Surf. Sci*. **1999**, *436*, 63.

(10) Pehrsson, P. E.; Mercer, T. W. *Surf. Sci*. **2000**, *460*, 49.

(11) Pehrsson, P. E.; Mercer, T. W. *Surf. Sci*. **2000**, *460*, 74.

(12) Mackey, B. L.; Russel, J. N.; Crowell, J. E., Jr.; Pehrsson, P. E.; Thoms, B. D.; Butler, J. E. *J. Phys. Chem B* **2001**, *105*, 3803.

(13) Klauser, R.; Chen, J.; Chuang, T.; Chen, L.; Shih, M.; Lin, J. *Surf. Sci*. **1996**, *356*, L410.

(14) de Theije, F. K.; Reedijik, M. F.; Arsic, J.; van Enckevort, W. J. P.; Vlieg, E. *Phys. Rev. B* **2001**, *64*, 85403.

(15) Ando, T.; Ishii, M.; Kamo, M.; Sato, Y. *J. Chem. Soc., Faraday Trans*. **1993**, *89*, 1783.

(16) Tamura, H.; Sugisako, K.; Yokoi, Y.; Takami, S.; Kubo, M.; Teraishi, K.; Miyamoto, A. *Phys. Rev. B*. **2000**, *61*, 11025.

(17) Foord, J. S.; Hian, L. C.; Jackman, R. B. *Diamond Relat. Mater*. **2001**, *10*, 701.

(18) Payne, M. C.; Teter, M. P.; Allan, D. C.; Arias, T. A.; Joannopoulos, J. D. *Rev. Mod. Phys*. **1992**, *64*, 1045.

(19) Vanderbilt, D. *Phys. Rev. B* **1990**, *41*, 7892.

(20) Bachelet, G. B.; Hamann, D. R.; Schluter, M. *Phys. Rev. B* **1982**, *26*, 4199.

(21) Monkhorst, H. J.; Pack, J. D. *Phys. Rev. B* **1976**, *13*, 5188.

(22) Polak, E. *Computational Methods in Optimization*; Academic: New York, 1971; p 56ff.

(23) Perdew, J. P.; Wang, Y. *Phys. Rev. B* **1992**, *45*, 13244.

(24) Pandey, K. C. *Phys. Rev. Lett*. **1981**, *47*, 1913.

(25) Bandis, C.; Pate, B. B. *Phys. Rev. B* **1995**, *52*, 12056.

(26) Himpsel, F. J.; Knapp, J. A.; VanVechten, J. A.; Eastman, D. E. *Phys. Rev. B* **1979**, *20*, 624.

(27) Lurie, P. G.; Wilson, J. M. *Surf. Sci*. **1977**, *65*, 476.

(28) Redhead, P. A. *Vacuum* **1962**, *12*, 203.

(29) Zheng, X. M.; Smith, P. V. *Surf. Sci*. **1992**, *262*, 219.

(30) Kern, G.; Hafner, J.; Kresse, G. *Surf. Sci*. **1996**, *366*, 464.

(31) Chin, R. P.; Huang, J. Y.; Shen, Y. R.; Chuang, T. J.; Seki, H.; Buck, M. *Phys. Rev. B* **1992**, *45*, 1522.

(32) Chin, R. P.; Huang, J. Y.; Shen, Y. R.; Chuang, T. J.; Seki, H. *Phys. Rev. B* **1995**, *52*, 5985.

(33) Matsumoto, S.; Setaka, N. *Carbon* **1979**, *17*, 485.

(34) Chu, C. J.; Pan, C.; Margrave, J. L.; Hauge, R. H. *Diamond Relat. Mater*. **1995**, *4*, 1317.

(35) Pate, B. B. *Surf. Sci*. **1986**, *165*, 83.

(36) Slevin, J.; Stirling, W. *Rev. Sci. Instrum*. **1981**, *52*, 1780.